Biochemical Pharmacology 79 (2010) 180–187

Contents lists available at ScienceDirect

Biochemical Pharmacology

journal homepage: www.elsevier.com/locate/biochempharm

Adenosine A_3 receptor-mediated cardioprotection against doxorubicin-induced mitochondrial damage

Avishag K. Emanuelov [a], Asher Shainberg [a], Yelena Chepurko [b], Doron Kaplan [c], Alex Sagie [d], Eyal Porat [d], Michael Arad [e], Edith Hochhauser [b,*]

[a] Gonda (Goldschmied) Medical Diagnostic Research Center, The Mina & Everard Goodman Faculty of Life Sciences, Bar-Ilan University, Ramat Gan, Israel
[b] Cardiac Research Laboratory, Felsenstein Medical Research Center, Rabin Medical Center, Petach Tikva, Tel Aviv University, Tel Aviv, Israel
[c] Israel Institute for Biological Research, Ness-Ziona, Israel
[d] Cardiology Department, Rabin Medical Center, Petach Tikva, Tel Aviv University, Tel Aviv, Israel
[e] Heart Institute, Sheba Medical Center, Tel Hashomer, Israel

ARTICLE INFO

Article history:
Received 4 June 2009
Accepted 6 August 2009

Keywords:
A_3 adenosine receptors
Ca^{2+} homeostasis
Cl-IB-MECA
Doxorubicin

ABSTRACT

Cardiotoxicity associated with doxorubicin (DOX) treatment limits the therapeutic efficiency of this drug against cancer. 2-Chloro-N(6)-(3-iodobenzyl)adenosine-5′-N-methyluronamide (Cl-IB-MECA), a selective agonist of A_3 adenosine receptor (A_3R), reduces DOX toxicity in newborn rat cultured cardiomyocytes. The study's aim was to determine whether the protection demonstrated by Cl-IB-MECA attenuates cardiac depression *in vivo*. In addition, we wished to examine whether this protective pathway affects the sarcoplasmic reticulum (SR) calcium uptake and release, as well as intramitochondrial Ca^{2+} accumulation induced by DOX.

Rats were injected every alternate day (6 times) with (1) saline, (2) 2.5 mg/kg i.p. DOX, (3) 33 μg/kg i.v. Cl-IB-MECA, (4) DOX + Cl-IB-MECA. Left ventricular functions were assessed by invasive (pressure) and non-invasive (echocardiography) techniques at the end of the injection period and 4 weeks later. Cytosolic and intramitochondrial calcium levels were measured with indo-1 and rhod-2 probes. SR Ca^{2+} content was determined by exposing cultured rat cardiomyocytes to caffeine.

Echocardiography data demonstrate left ventricular wall thinning (23%), an increase in the end systolic dimension (170%) and decreased fractional shortening ($35 \pm 5\%$ vs. $54 \pm 5\%$, $p < 0.01$) in DOX-treated animals, compared to the control group. DOX increased Ca^{2+} levels in the cytosol and in mitochondria by diminishing the SR Ca^{2+} uptake. Pretreatment with Cl-IB-MECA attenuated left ventricular dysfunction, improved SR calcium storage capacity and prevented mitochondrial Ca^{2+} overload.

We conclude that the adenosine A_3 receptor agonist is effective *in vivo* against DOX cardiotoxicity via the restoration of Ca^{2+} homeostasis and prevention of mitochondrial damage that occurs as a result of Ca^{2+} overload.

1. Introduction

The anthracycline antibiotic doxorubicin (DOX), also called adriamycin, and its congener, Daunorubicin (Daunomycin), have been used for over 30 years to treat a variety of malignancies, including leukemias, lymphomas and solid tumors [1]. The clinical use of DOX is limited because of its dose-dependent cardiotoxicity which is unrelated to its cytotoxic effect and leads to dilated cardiomyopathy and severe heart failure [2]. Acute cardiotoxicity develops in the course and shortly after the initiation of DOX treatment, manifested by arrhythmia, contractile dysfunction and hypotension. This form of toxicity can be avoided by limiting the cumulative drug dose to below 500 mg/m^2. In contrast, subacute and chronic toxicity may develop months to years after completion of chemotherapy and produce life-threatening dilated congestive cardiomyopathy [3]. Anthracycline-induced cardiotoxicity is observed in up to 20% of patients receiving the drug. Since DOX has remarkable antitumor activity, novel methods to reduce or prevent the detrimental side effects are expected to increase its effectiveness in anti-cancer therapy [4].

The cardiac toxicity of DOX results in typical histopathological changes in heart sections [2]. The mechanism is not yet completely understood. It has been suggested that formation of reactive oxygen species, apoptosis, inhibited expression of cardiomyocytes-specific genes, and altered molecular signaling are contributors to DOX-induced cardiomyopathy [5].

* *Corresponding author*. Tel.: +972 3 9376284; fax: +972 3 9211478.
E-mail addresses: shaina@mail.biu.ac.il (A. Shainberg), doronk@iibr.gov.il (D. Kaplan), asgie@clalit.org.il (A. Sagie), michael.arad@sheba.health.gov.il (M. Arad), hochhaus@post.tau.ac.il (E. Hochhauser).

0006-2952/$ – see front matter © 2009 Elsevier Inc. All rights reserved.
doi:10.1016/j.bcp.2009.08.010

We have previously shown in cultured cardiomyocytes that activation of adenosine A_3 receptor (A_3R) by the highly selective agonist 2-chloro-N^6-(3-iodobenzyl)adenosine-5′-N-methyluronamide (Cl-IB-MECA) induces resistance of the cells to DOX. It has been demonstrated that activation of the A_3R before and during exposure to the drug evoked a decrease in intracellular calcium overloading, prevented abnormality in Ca^{2+} transients, restrained generation of free-radicals and lipid peroxidation. In addition, attenuation of mitochondrial damage and maintaining of ATP production were shown in cells treated with DOX via activation of A_3R. Cardioprotection caused by Cl-IB-MECA was blocked with the selective antagonist MRS1523, confirming protective response via A_3 receptor [6]. The cardioprotective action of A_3R stimulation was further characterized by elucidation of progressive structural (cellular, mitochondrial and lysosomal) and functional (K_{ATP} channels, mitochondrial membrane potential) changes elicited in cardiomyocytes upon exposure to DOX and A_3R agonist Cl-IB-MECA [7].

In the present study, we demonstrate that A_3R stimulation by Cl-IB-MECA is effective against DOX-induced cardiotoxicity *in vivo*. We also describe a mechanism of protection in which Cl-IB-MECA supports the activity of SR Ca^{2+} ATPase, thereby preventing intracellular Ca^{2+} accumulation and mitochondrial calcium overload.

2. Materials and methods

2.1. In vivo experiments

2.1.1. Animals

All experiments were carried out in accordance with the guidelines of the Animal Care and Use Committee of the Felsenstein Medical Research Center and Tel Aviv University, with the Guide for the Care and Use of Laboratory Animals published by the US National Institutes of Health (NIH Publication No. 85–23, revised 1996).

2.1.2. Chemicals

All chemicals were purchased from Sigma Chemical Co. (St. Louis, MO) unless stated otherwise.

Male Sprague–Dawley rats (250–300 g, 3 months old) were injected intraperitoneally with DOX 2.5 mg/kg every second day for a period of two weeks (henceforth, injection period), a total of 6 times, reaching a cumulative dose of 15 mg/kg as previously described [4]. Cl-IB-MECA (33 μg/kg) was injected to the tail vein 15 min before DOX injection. Rats were injected every alternate day (6 times) with (1) saline, (2) DOX, (3) Cl-IB-MECA, (4) DOX + Cl-IB-MECA (a total of four groups), $n = 8–10$ animals in each group. A pilot study of different Cl-IB-MECA concentrations (10–100 μg/kg) was conducted to select the most effective concentration for our experimental protocol. After the injection period (Inj P) animals were monitored for a period of 3–4 weeks, henceforth, observation period (Obs P). DOX was given i.p. and Cl-IB-MECA was administered i.v. to prevent intraperitoneal interactions between both drugs when administered simultaneously.

2.1.3. Hemodynamic measurements

Animals were anaesthetized with a mixture of 8 mg/100 ml ketamine and 5 mg/100 ml xylazine. The right carotid artery was isolated and a polyethylene tube (PE 50) was inserted through it into the left ventricular cavity and connected to a pressure transducer filled with saline (Mennen Medical, Inc., Clarence, NY, USA) using AT-CODAS Software (Dataq Instr. Inc., Akron, OH, USA). Left ventricular systolic pressure (LVSP) was monitored only once at four weeks post-injection period before sacrifice [8].

2.1.4. Echocardiography

Animals were anesthetized by inhalation of isoflurane. Two-dimensional (2D) guided M-mode echocardiography was performed using an echocardiogram (Philips, Sonos 5500, USA) equipped with a S12 MHz phased-array transducer. The parasternal short-axis view of the hearts was viewed in a 2D image. The M-mode cursor was then positioned perpendicular to the interventricular septum and the posterior wall of the LV at the level of the papillary muscles. An M-mode image was obtained at a sweep speed of 100 mm/s. Diastolic and systolic LV wall thickness, LV end-diastolic diameter (LVEDD), and LV end-systolic diameter (LVESD) were measured. The percent LV fractional shortening (%FS) was calculated as $[(LVEDD - LVESD)/LVEDD] \times 100$. Echocardiography was performed at base line, on completion of injections and four weeks post-injection period (8).

2.2. In vitro experiments

2.2.1. Cell culture

Rat hearts (2–3 days old) were removed under sterile conditions and washed 3 times in phosphate buffered saline (PBS) to remove excess blood cells. The hearts were minced and then gently agitated in a solution of proteolytic enzymes, RDB (Biological Institute, Ness-Ziona, Israel), prepared from a fig tree extract [9]. RDB was diluted 1:100 in Ca^{2+}- and Mg^{2+}-free PBS at 25 °C for a few cycles of 10 min each, as previously described [10]. Dulbecco's modified Eagle's medium, supplemented with inactivated 10% horse serum (Biological Industries, Beit Haemek, Israel) and 0.5% chick embryo extract, were added to supernatant suspensions containing dissociated cells. The mixture was centrifuged at $300 \times g$ for 5 min. The supernatant phase was discarded, and the cells were resuspended in the same medium. The suspension of the cells was diluted to 1.0×10^6 cells/ml, and 1.5 ml of the suspension was placed in 35-mm collagen/gelatin-coated plastic culture dishes or cover glasses. The cultures were incubated in a humidified atmosphere of 5% CO_2, 95% air at 37 °C. Confluent monolayers exhibiting spontaneous contractions were developed in culture within 2 days. All experiments were performed between days 5 and 7 in culture.

2.2.2. Intracellular Ca^{2+} measurements

Intracellular free calcium $[Ca^{2+}]_i$ from individual cardiomyocytes was measured using the indicator indo-1-AM under a Zeiss epi-fluorescent inverted microscope. The ratiometric methods for the quantification of the results have been described previously [11]. Cardiomyocytes grown on a coverglass were incubated with 2 μM indo-1-AM and 1.5 μM pluronic acid for 30 min in PBS with glucose (25 mM) at 25 °C. After incubation, the cells were rinsed twice with glucose-enriched PBS and transferred to a chamber on the microscope. Indo-1 loaded cells were excited at 355 nm and the emitted light then split by a dichroic mirror into two photomultipliers (Hamamatsu, Japan), with input filters at 410 and 490 nm for indo-1. The fluorescence ratio (R) of 410 nm/490 nm, which is proportional to $[Ca^{2+}]_i$, was implemented to the SAMPLE program. Cells grown on coverslips were treated with DOX (20 μM) and Cl-IB-MECA (100 nM). A high concentration of DOX was used to accomplish immediate effect of DOX on intracellular Ca^{2+}. The time integral of Ca^{2+} influx was determined as the area under the curve via the SAMPLE program, which gives the integral during any specified time window. The baseline offset, measured at the diastolic level, was subtracted from this value. The time window was the same for each experiment.

2.2.3. Measurements of mitochondrial Ca^{2+}

Mitochondrial calcium ion concentration was estimated by rhod-2 fluorescence using the method previously described [8,12].

Table 1
Changes of various physiological parameters induced by Cl-IB-MECA on DOX toxicity.

		Control	Cl-IB-MECA	DOX	DOX + Cl-IB-MECA
A	Mortality	0%	0%	30%	0%
	Ascitic fluid	0	0	7–14ml	0
	Body weight (BW) (g)	350 ± 49	328 ± 52	266 ± 15♣	281 ± 11
	Heart weight (H) (g)	0.97 ± 0.1	0.94 ± 0.15	0.86 ± 0.04	0.84 ± 0.08
	H/BW ratio ($\times 10^2$)	0.27	0.27	0.34*	0.28#
B	LVSP	121 ± 19	130 ± 20	130 ± 14	116 ± 14

(A) The effect of Cl-IB-MECA on DOX-induced changes in mortality, ascites, body weight (BW), heart weight (H) and H/BW weight ratio. ♣$P < 0.05$ vs. control group; *$P < 0.001$ vs. control group; #$P < 0.001$ vs. DOX group, $n = 8–10$ animals in each group.
(B) The effect of Cl-IB-MECA on DOX-induced change in left ventricular systolic blood pressure (LVSP). Values are expressed as mean ± S.D.

Cardiac cells grown on coverslips were treated with DOX and Cl-IB-MECA for 18 h and for an additional 24 h with drug-free medium. To accomplish a long-term effect on mitochondrial Ca^{2+}, we used lower concentrations of DOX (2 μM). After treatment, cells were exposed to rhod-2-AM (10 μM), dissolved in PBS, at 4 °C, for 120 min and then washed and transferred to 37 °C for an additional 120 min. Rhod-2 fluorescence, representing mitochondrial calcium, was elicited by excitation at 540 nm and emission was measured at a wavelength of 590 nm [8].

2.2.4. Statistical analysis

Results are expressed as means ± standard deviation. A statistical difference between the groups was assessed using the analysis of variance (ANOVA) with repeated measurements using the multiple comparison option of Duncan, $p < 0.05$ was considered significant.

3. Results

3.1. Morbidity and mortality

At baseline, body and heart weight were similar in all groups. There was no mortality throughout the two-week injection period. During the 4-week observation period 6 out of 20 (30%) in DOX-treated rats died (Table 1A). All animals in the DOX-treated group developed congestive heart failure manifested by marked ascites accumulating to 7–14 ml. No ascites was observed in the Cl-IB-MECA + DOX-treated group or the control group (Table 1A). Four weeks after the injection period, DOX and DOX + Cl-IB-MECA-treated animals did not gain as much weight as the control group. However, Cl-IB-MECA + DOX attenuated the decrease in body weight compared to DOX alone ($p < 0.05$ vs. DOX), resulting in a similar heart to body weight ratio compared to controls (Table 1A).

3.2. Hemodynamic measurements

No differences in left ventricular systolic pressures were observed between the groups when measured following the observation period (Table 1B). LV end diastolic pressure was in the range of 1–5 mmHg in all tested groups.

3.3. Echocardiographic assessment of left ventricle performance

After the injection period, left ventricular end-diastolic and end-systolic areas (LVEDA and LVESA, respectively) were identical in DOX-treated and control groups. During the four weeks of the observation period, the left ventricle progressively dilated, fractional shortening (FS) decreased (Fig. 1A and B) and the LV walls became significantly thinner in the DOX-treated group

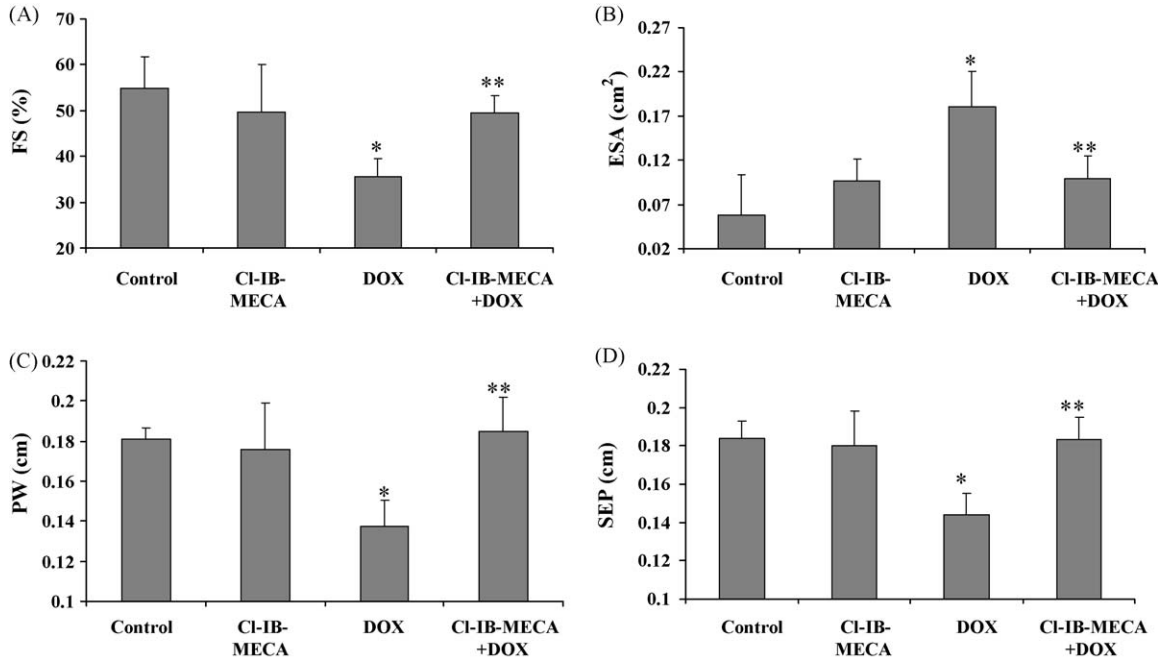

Fig. 1. Echocardiographic studies four weeks post-DOX injection. Fractional shortening (FS) left ventricular end systolic area (ESA) (A and B), changes in the left ventricular posterior wall (PW) and septum (SEP) thickness (C and D) in all groups. Values represent means ± S.D.
*$P < 0.001$ vs. control group.
**$P < 0.001$ vs. DOX group.

Table 2
The effect of Cl-IB-MECA on DOX-induced change in heart rate (HR).

Treatments	HR (bpm)		
	Baseline	Inj P	Obs P
Control	281 ± 12	280 ± 11	280 ± 11
Cl-IB-MECA	283 ± 14	286 ± 15	286 ± 15
DOX	280 ± 8	225 ± 4*	220 ± 10*
Cl-IB-MECA + DOX	276 ± 13	271 ± 20	271 ± 20

Injection period, Inj P; observation period, Obs P.
All values are expressed as mean ± S.D.
* $P < 0.05$ vs. control group, $n = 8–10$ animals in each group.

compared with controls (Fig. 1C and D). The addition of Cl-IB-MECA to the DOX treatment attenuated left ventricular dilatation and wall thinning. This group demonstrated significantly improved FS compared to the DOX-treated group (Fig. 1A). No differences in heart rate (HR) were observed between the groups at baseline. After the injection period, as well as the observation period heart rate of DOX-treated animals was lower (20%) when compared to controls. Cl-IB-MECA treatment prevented a decrease in the heart rate (Table 2).

3.4. The effect of doxorubicin on Ca^{2+} transients in cultured cardiomyocytes

Intracellular free calcium concentration was estimated by indo-1 fluorescence. Control myocytes demonstrated spontaneous, regular beating activity and $[Ca^{2+}]_i$ transients in indo-1-loaded cells for at least three hours (Fig. 2A). We have previously shown that adding 20 μM DOX (for 1 h) caused $[Ca^{2+}]_i$. elevation [6]. In this study, we have demonstrated that pretreatment with 10 μM verapamil, a concentration that blocks L-type calcium channels, did not prevent the increase in calcium levels $[Ca^{2+}]_i$ (Fig. 2B and C), suggesting that $[Ca^{2+}]_i$ elevation after DOX administration is not via L-type Ca^{2+} channels. Moreover, even in the absence of extracellular Ca^{2+}, using calcium-free medium and EGTA (calcium chelator), treatment with DOX caused $[Ca^{2+}]_i$ elevation (Fig. 2D and E). Pretreatment with 100 μM ryanodine, a concentration that blocks the ryanodine receptor channels (RyR), prevented DOX-induced $[Ca^{2+}]_i$ elevation (Fig. 3). Thus, these results indicate that the rise in $[Ca^{2+}]_i$ after DOX treatment, originates from the sarcoplasmic reticulum (SR) and involves Ca^{2+} release through RyR channel.

3.5. The effect of A_3 adenosine receptor activation on $[Ca^{2+}]_i$ in cultured cardiomyocytes after DOX treatment

Exposure of cardiomyocytes to 10 mM caffeine causes Ca^{2+} release from the SR, and tests the Ca^{2+} content in the SR. Application of caffeine after 2 h of 20 μM DOX treatment, produced no additional elevation of $[Ca^{2+}]_i$, indicating that DOX treatment had already depleted SR calcium content (Fig. 4A). However, cardiomyocytes treated with the A_3R agonist 100 nM Cl-IB-MECA, together with DOX preserved the expected elevation in Ca^{2+} release after the caffeine test, despite DOX treatment. Treatment with this A_3R agonist, restored Ca^{2+} oscillations, which was comparable to controls (Fig. 4B). We have previously shown that Cl-IB-MECA's protective effect was neutralized when the A_3R antagonist, MRS 1523, was administered concomitantly with Cl-IB-MECA [6]. To test the ability of Cl-IB-MECA to preserve SR Ca^{2+} uptake, we blocked SERCA2a activity by the administration of 100 nM thapsigargin. There was no further Ca^{2+} release in response to caffeine in cells pretreated with thapsigargin and Cl-IB-MECA

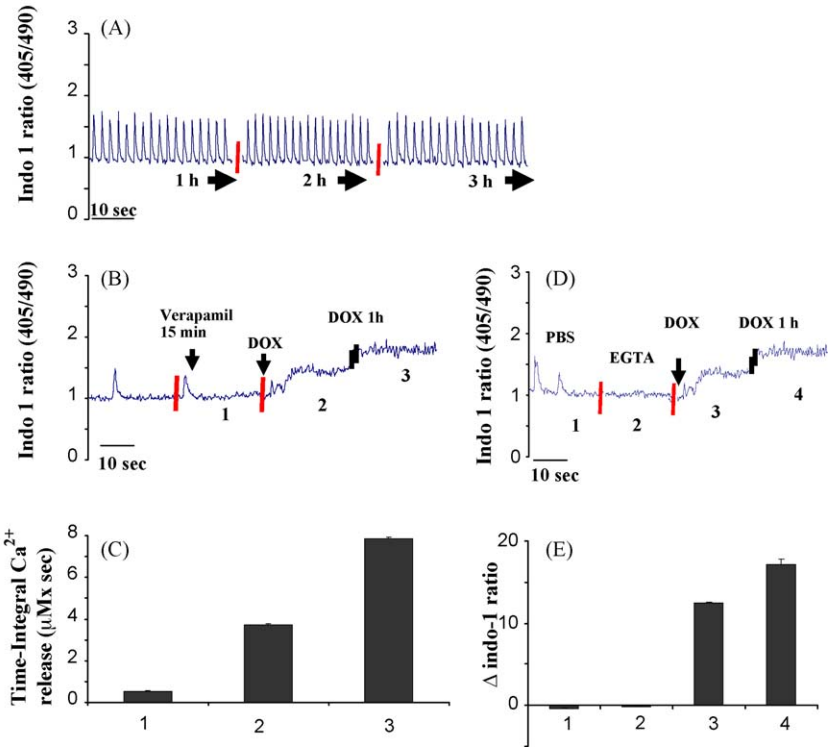

Fig. 2. The effect of DOX on intracellular calcium concentration. (A) Stability of intracellular calcium level and $[Ca^{2+}]_i$ transients in control cardiomyocytes over a period of 3 h. (B) Calcium elevation as response to 20 μM DOX (arrow) was not inhibited by 10 μM verapamil (L-type calcium channel blocker, arrow). (C) A histogram summarizing the indo-1 fluorescence ratio minus baseline ratio in control and cells treated with 10 μM verapamil (1), after 20 μM DOX (2), after 1 h with 20 μM DOX (3). (D) Calcium elevation following 20 μM DOX (arrow) was not inhibited by calcium-free PBS^{2-} containing 1 mM EGTA. (E) A histogram summarizing the indo-1 fluorescence ratio minus baseline ratio in control and cells in PBS^{2-} (1), after the addition of 1 mM EGTA (2), addition of 20 μM DOX (3), and after 1 h with 20 μM DOX (4).

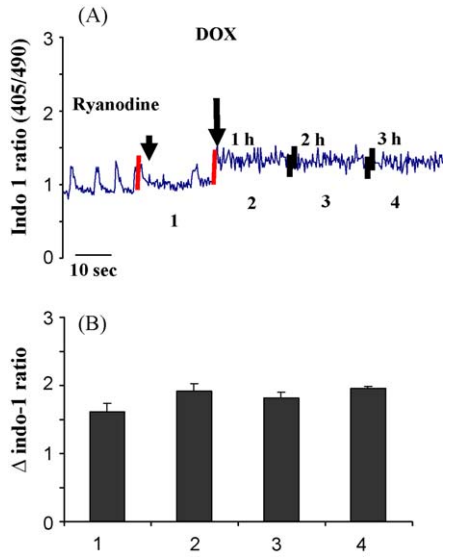

Fig. 3. The effect of ryanodine on $[Ca^{2+}]_i$ in DOX-treated cardiomyocytes. (A) Calcium elevation following 20 μM DOX (arrow) was almost completely inhibited by 100 μM ryanodine (arrow, a concentration that blocks ryanodine receptor). (B) Histogram summarizing the indo-1 fluorescence ratio minus baseline ratio in control and after treated with 100 μM ryanodine (1), 1 h after the application of 20 μM DOX (2), 2 h after DOX (3), 3 h after DOX (4). Data are means ± S.D. from 10 experiments.

(Fig. 4C and D) as was demonstrated in the effect of caffeine following DOX in Fig. 4A. Cumulatively, these results suggest that DOX impairs SERCA2a activity, while Cl-IB-MECA activates SERCA2a thereby restoring Ca^{2+} pumping into the SR and preventing the rise in cytosolic calcium.

3.6. Mitochondrial Ca^{2+} concentration vs. $[Ca^{2+}]$

The mitochondrial Ca^{2+} concentration was estimated from rhod-2 fluorescence. Treatment with 2 μM DOX for 18 h following 24 h incubation in drug-free medium resulted in a significant elevation of intramitochondrial Ca^{2+} and a high level of $[Ca^{2+}]_i$ (Fig. 5A–C and G). The application of 100 nM Cl-IB-MECA 15 min before DOX treatment prevented the elevation in mitochondrial Ca^{2+}, preserved $[Ca^{2+}]_i$ levels and normal oscillations of Ca^{2+} (Fig. 5D, H).

4. Discussion

Many therapies have been proposed to prevent DOX cardiotoxicity. DOX has proven to be a double-edged sword because it may cause cardiomyopathy that often leads to congestive heart failure. It has been hypothesized that better understanding of the mechanisms underlying DOX cardiotoxicity will help prevent heart failure associated with such treatment without compromising its antineoplastic activity, thereby expanding the therapeutic window of this potent chemotherapy [4]. In this study, we found that application of Cl-IB-MECA prior to DOX treatment prevented the elevation in mitochondrial Ca^{2+} caused by DOX alone, enabling normal mitochondrial function.

A variety of approaches aimed at preventing or mitigating the cardiotoxicity of DOX have been tried but, so far, the ability of these treatments to protect the heart from DOX damage has been limited. Because of the role of reactive oxygen species in doxorubicin cardiotoxicity, attention has been focused on oxygen radical scavengers as cardioprotective agents [13]. Iron chelators, such as dextrazoxane, became clinically available but their use may be limited by side effects and the possibility of reducing the anti-cancer effect [14,15]. Therapies addressing the inflammatory component subsequent to oxidative stress [16], mitochondrial dysfunction [17] and apoptosis [18] have been considered and showed promising results in *in vitro* and *in vivo* models.

DOX-induced cardiomyopathy is well documented in various animal models and is comparable to humans [3,4,19,20]. DOX-induced cardiomyopathy has been previously described in the rat model [21–23]. However, the dose of DOX, i.e. from 1 mg/kg body weight to 2.5 mg/kg, the frequency and the route of administration, i.e. once a week or once every 3 weeks, subcutaneously, i.p. or i.v. and the total duration of treatment, i.e. from 6 to 20 weeks, varied. Using our techniques, the rats developed subacute cardiac

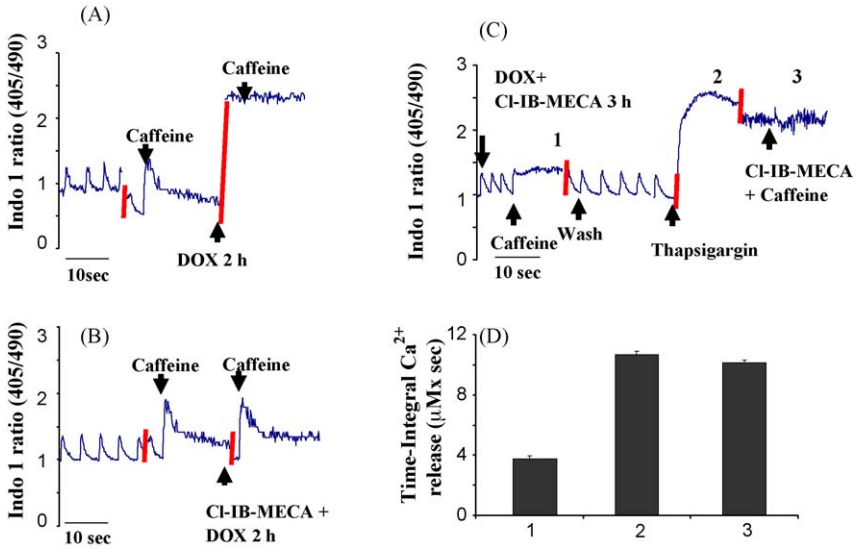

Fig. 4. Effect of DOX on SR calcium content: (A) Effect of 10 mM caffeine (arrow) on $[Ca^{2+}]_i$ in myocardial cells after application of 20 μM DOX for 2 h. (B) Effect of 10 mM caffeine on $[Ca^{2+}]_i$ in myocardial cells after application of Cl-IB-MECA + 20 μM DOX for 2 h (arrow). (C) Effect of thapsigargin (arrow) on $[Ca^{2+}]_i$ in myocardial cells after treatment with Cl-IB-MECA + 20 μM DOX (arrow) for 3 h and then application of 10 mM caffeine (arrow). (D) Histogram summarizing the indo-1 fluorescence ratio minus baseline ratio in control and after the addition of 10 mM caffeine following treatment with Cl-IB-MECA + 20 μM DOX for 3 h (1), after the addition of 100 nM thapsigargin (2), after the addition of 10 mM caffeine (3). Data are means ± S.D. from 10 experiments.

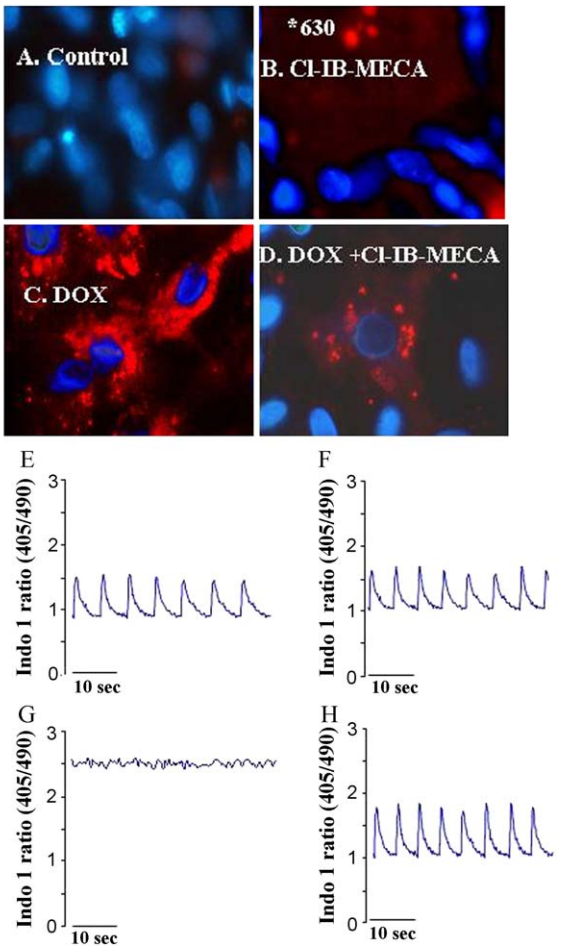

Fig. 5. Fluorescence images illustrating the effect of Cl-IB-MECA and DOX on mitochondrial Ca^{2+} vs. intracellular Ca^{2+}. Mitochondrial Ca^{2+} was stained with rhod-2 and the nuclei with Hoechst 33342 (A–D). Simultaneous intracellular $[Ca^{2+}]_i$ measured with indo-1 appears in E–H. (A) Control cells, (B) cells treated with 100 nM Cl-IB-MECA, (C) cells treated with 2 μM DOX for 18 h and then left for 24 h in a drug-free medium, (D) cells treated with 100 nM Cl-IB-MECA + 2 μM DOX, (E) control cells, (F) cells treated with Cl-IB-MECA, (G) DOX-treated cells as in C and (H) DOX and Cl-IB-MECA-treated cells as in D.

failure after 2.5 mg/kg DOX, administered i.p. 3 times a week for only two weeks (cumulative dose of 15 mg/kg). On completion of injections, animals from all groups had no dyspnea, ascites, mortality or differences in hemodynamic measurements. At four weeks post-treatment, rats in the DOX group developed left ventricular dysfunction and suffered from ascites, dyspnea and 30% mortality. Hemodynamic measurements revealed reduced heart rate and FS only in the DOX group. Compared to the rabbit model where only 7/16 animals (44%) had a reduction in ejection fraction [24], the rat model described here is very reliable with a high incidence of cardiomyopathy and low mortality during the treatment phase but increased heart failure, morbidity and mortality during the ensuing 4-weeks period. The feasibility of echocardiography, used in this study to assess the cardiac function in DOX-induced cardiomyopathy in rats, has previously been demonstrated [25]. The A_3 adenosine receptor agonist, Cl-IB-MECA, prevented the decrease in cardiac functions, ascites and mortality.

The body weight of the animals at the beginning of the study was 225–250 g. This is usually the average weight of our male Sprague–Dawley rats at the age of three months. They did gain weight during the six weeks of the study and reached an average of 350 ± 49 g. In this project, we decided to work with young animals, in order to follow their growth and survival. The fact that doxorubicin prevented the progression of both heart weight and body weight has already been documented [4,26]. Although the DOX + Cl-IB-MECA-treated animals did not gain as much weight as the control group, they gained more weight than the DOX alone group. These results point to Cl-IB-MECA's ability to attenuate the decrease in weight loss, indicating this A_3R agonist's possible influence in a variety of positive elements required for the rats' well-being.

We have previously demonstrated the cardioprotective effects of a newly identified adenosine A_3 receptor agonist in the model of DOX-induced cardiotoxicity in culture [6,7]. The protective effect of the A_3R agonist is abolished by the A_3R antagonist MRS 1523 [6], supporting the notion of cardioprotection via activation of A_3 adenosine receptors. It was established that activation of A_3R before and during exposure to the drug evoked a decrease in intracellular calcium overloading, prevented abnormalities in Ca^{2+} transients, and restrained generation of free-radicals and lipid peroxidation. In addition, attenuation of mitochondrial damage, as revealed by protection of the terminal link (COX complex) of the respiratory chain, and maintaining of ATP production, was observed in cells treated with DOX through A_3R activation. Dysfunction of mitochondria, manifested by a decrease in ATP synthesis, which occurs in DOX-treated cardiomyocytes [6,7], led us to postulate that the mitochondria are the primary target for DOX-induced cardiac toxicity. DOX intercalates with DNA and causes oxidative damage to nuclear and mitochondrial DNA [7,26,27]. Mitochondrial dysfunction is a hallmark of DOX cardiotoxicity [5]. DOX induces defects at the different stages of cardiac energy metabolism, including the reduction of the oxidative capacity of the mitochondria, changes in the profile of energy substrate utilization and disturbing the energy transfer between sites of energy production and consumption [5]. Because mitochondrial Ca^{2+} overload leads to mitochondrial dysfunction, we addressed the question whether Cl-IB-MECA could attenuate the rise in the mitochondrial calcium level caused by DOX treatment. After treatment with DOX we observed a significant elevation of intramitochondrial Ca^{2+} level. Application of Cl-IB-MECA prior to DOX treatment prevented the elevation in mitochondrial Ca^{2+} (Fig. 5).

Calcium overload was the first mechanism introduced to explain DOX cardiotoxicity [28]. The complex nature of the modulation of myocardial Ca^{2+} handling following DOX is now recognized [29]. We and others have shown that DOX induces a spontaneous leak of Ca^{2+} from the SR leading to inadequate Ca^{2+} release for contraction [30,31]. In the current work, we investigated the mechanism of intracellular calcium increase in cells after DOX treatment. We observed that neither L-type calcium channels blockade nor extracellular calcium-free medium prevented the rise in cytosolic calcium after DOX administration. When we blocked the RyR channels with ryanodine (100 μM), no rise in cytosolic calcium was found even after 3 h of DOX treatment. Thus, DOX increases $[Ca^{2+}]_i$ by releasing it from the SR via RyR (Fig. 3). Based on these results, we assessed the levels of calcium in SR after DOX application and their relation to SERCA2a activity, using thapsigargin. DOX causes calcium depletion from the SR. Cells treated with Cl-IB-MECA + DOX, demonstrated a normal reaction to caffeine releasing test, indicating preserved SR calcium stores (Fig. 4A and B). When SERCA2a activity was inhibited with thapsigargin, there was no response to caffeine even when the cells were treated with Cl-IB-MECA. Thus, we conclude that DOX inhibits Ca^{2+} accumulation in the SR while Cl-IB-MECA activates SERCA2a, restores SR calcium and prevents a rise in cytosolic calcium after DOX treatment. We suggest that the high local $[Ca^{2+}]_i$ produced by DOX, causes mitochondrial Ca^{2+} overload leading to a large spectrum of alterations in the cardiac energy metabolism and

eventually to cell death. Although the heart has extraordinary plasticity in relation to calcium handling, the cardiotoxicity of DOX remains detrimental. Transgenic mice could also be used to investigate the role of SERCA in DOX cardiotoxicity. Mice lacking SERCA remain viable for 7 weeks with less than 20% of control levels of SERCA2, because they utilize compensatory mechanisms such as changes in the properties of the myofilaments and possibly also cytosolic Ca^{2+} buffers in order to maintain functionality [32,33]. On the other hand, overexpression of A_3R *in vivo*, was accompanied by a dose-dependent AV block and pronounced sinus nodal dysfunction. Activation of A_3R is known or supposed to enhance SERCA function in various tissues, and in particular in cardiomyocytes [34]. In our work, we administered Cl-IB-MECA prior to DOX treatment and we assume no change of any gene took place. Our aim was to find new ways to abolish DOX cardiotoxicity without interfering with its antitumor effect. It has been demonstrated that A_3R agonists were found to induce tumor growth inhibition, both *in vitro* and *in vivo* via the modulation of the Wnt and the NF-kappaB signaling pathways [35]. If the agonist is considered an antitumor agent, the possibility that it will diminish DOX's antitumor effect is unlikely. When it was tested in a culture of PC-3 cells (human cancer cells of the prostate) DOX inhibited thymidine incorporation. Cl-IB-MECA did not prevent the inhibition by DOX, indicating that the agonist did not block the antitumor effect of DOX (data not shown). Nevertheless, *in vivo* experiments on rats carrying tumors and treated with doxorubicin + Cl-IB-MECA should be tested to investigate whether the cardioprotection persists without a diminished antitumor effect. This would strongly support the potential value of the A_3 agonist in clinical use for cardioprotection in a chemotherapeutic setting. A simplified overview of one of the mechanisms responsible for Ca^{2+} overload after DOX treatment, and the protective effect of A_3R activation are presented in Fig. 6.

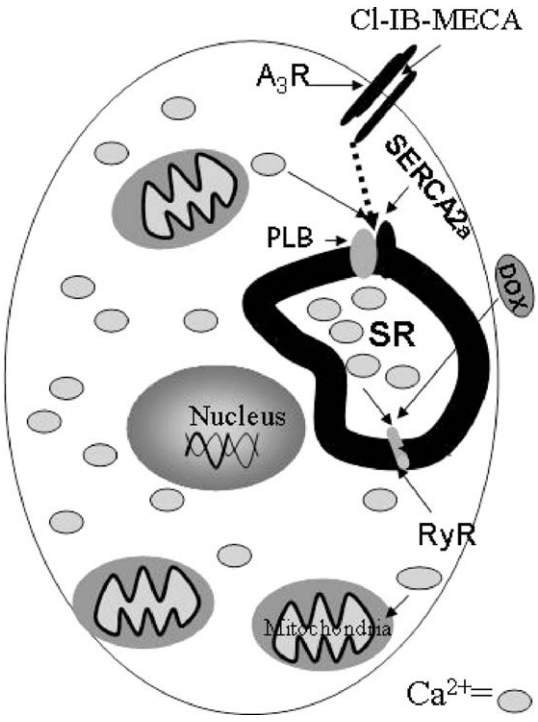

Fig. 6. Illustration summarizing the mechanisms responsible for Ca^{2+} overload after DOX treatment, and the protective effect induced by activation of A_3R. DOX induces Ca^{2+} release from the SR via the calcium release channels ryanodine receptor (RyR). The elevated $[Ca^{2+}]_i$ causes mitochondrial Ca^{2+} overload leading to a large spectrum of drawbacks in the cardiac energy metabolism and eventually to cell death. Cl-IB-MECA, A_3R agonist, activates the SR Ca^{2+}-ATPase (SERCA2a) thereby preventing the interaction between SR Ca-ATPase (SERCA2a) with phospholamban (PLB), hence preventing intracellular Ca^{2+} accumulation and mitochondrial calcium overload, thus protecting the cardiomyocytes.

We conclude that cardioprotection against DOX cardiotoxicity may be achieved by A_3R agonist, Cl-IB-MECA, through restoration of Ca^{2+} pumping into the SR, thereby preventing cytosolic and mitochondrial Ca^{2+} overload. Treatment with A_3R agonist may offer a novel approach to reduce doxorubicin injury. Further *in vivo* studies are warranted to investigate their long-term efficacy and compatibility with the antitumor activity of doxorubicin. We can only speculate that cardiomyocyte cell survival pathways as a result of DOX treatment are similar to that of cardioprotection from ischemia. In both cases the stress induces Ca^{2+} elevation and therefore Cl-IB-MECA prevents the rise of Ca^{2+}, thus protecting the cardiac cells.

Sources of funding

This research study was conducted through the generous support of The Adar Program for the Advancement of Research in Heart Function and the Horowitz Foundation at Bar-Ilan University.

Acknowledgments

We are indebted to Dr. T. Zinman and Ms. A. Isak for their valuable technical assistance.

References

[1] Lum BL, Gosland MP, Kaubisch S, Sikic BI. Molecular targets in oncology: implications of the multidrug resistance gene. Pharmacotherapy 1993;13:88–109 [review].
[2] Takemura G, Fujiwara H. Doxorubicin-induced cardiomyopathy from the cardiotoxic mechanisms to management. Prog Cardiovasc Dis 2007;49:330–52.
[3] Outomuro D, Grana DR, Azzato F, Milei J. Adriamycin-induced myocardial toxicity: new solutions for an old problem? Int J Cardiol 2007;117:6–15.
[4] Robert J. Long-term and short-term models for studying anthracycline cardiotoxicity and protectors. Cardiovasc Toxicol 2007;7:135–9.
[5] Tokarska-Schlattner M, Zaugg M, Zuppinger C, Wallimann T, Schlattner U. New insights into doxorubicin-induced cardiotoxicity: the critical role of cellular energetics. J Mol Cell Cardiol 2006;41:389–405.
[6] Shneyvays V, Mamedova L, Zinman T, Jacobson K, Shainberg A. Activation of A_3 adenosine receptor protects against doxorubicin-induced cardiotoxicity. J Mol Cell Cardiol 2001;33:1249–61.
[7] Shneyvays V, Mamedova L, Korkus A, Shainberg A. Cardiomyocyte resistance to doxorubicin mediated A_3 adenosine receptor. J Mol Cell Cardiol 2002;34:493–507.
[8] Yitzhaki S, Shainberg A, Cheporko Y, Vidne BA, Sagie A, Jacobson KA, Hochhauser E. Uridine-5'-triphosphate (UTP) reduces infarct size and improves rat heart function after myocardial infarct. Biochem Pharmacol 2006;72:949–55.
[9] Shneyvays V, Nawrath H, Jacobson KA, Shainberg A. Induction of apoptosis in cardiac myocytes by an A_3 adenosine receptor agonist. Exp Cell Res 1998;243:383–97.
[10] Safran N, Shneyvays V, Balas N, Jacobson KA, Shainberg A. Cardioprotective effects of adenosine A_1 and A_3 receptor activation during hypoxia in isolated rat cardiac myocytes. Mol Cell Biochem 2001;217:143–52.
[11] Fixler D, Tirosh R, Zinman T, Shainberg A, Deutsch M. Differential aspects in ratio measurements of $[Ca^{2+}]_i$ relaxation in cardiomyocyte contraction following various drug treatments. Cell Calcium 2002;31:279–87.
[12] Jo H, Noma A, Matsuoka S. Calcium-mediated coupling between mitochondrial substrate dehydrogenation and cardiac workload in single guinea-pig ventricular myocytes. J Mol Cell Cardiol 2006;40:394–404.
[13] Cole MP, Chaiswing L, Oberley TD, Edelmann SE, Piascik MT, Lin SM, et al. The protective roles of nitric oxide and superoxide dismutase in adriamycin-induced cardiotoxicity. Cardiovasc Res 2006;69:186–97.
[14] Sterba M, Popelová O, Simunek T, Mazurová Y, Potácová A, Adamcová M, et al. Cardioprotective effects of a novel iron chelator, pyridoxal 2-chlorobenzoyl hydrazone, in the rabbit model of daunorubicin-induced cardiotoxicity. J Pharmacol Exp Ther 2006;319:1336–47.
[15] Yeh ET, Tong AT, Lenihan DJ, Yusuf SW, Swafford J, Champion C, et al. Cardiovascular complications of cancer therapy: diagnosis, pathogenesis, and management. Circulation 2004;109:3122–31.
[16] Bruynzeel AM, Abou El Hassan MA, Schalkwijk C, Berkhof J, Bast A, et al. Anti-inflammatory agents and monoHER protect against DOX-induced cardiotoxicity and accumulation of CML in mice. Br J Cancer 2007;96:937–43.

[17] Roffe L, Schmidt K, Ernst E. Efficacy of coenzyme Q10 for improved tolerability of cancer treatments: a systematic review. J Clin Oncol 2004;22:4418–24.
[18] Fisher PW, Salloum F, Das A, Hyder H, Kukreja RC. Phosphodiesterase-5 inhibition with sildenafil attenuates cardiomyocyte apoptosis and left ventricular dysfunction in a chronic model of doxorubicin cardiotoxicity. Circulation 2005;111:1601–10.
[19] Singal PK, Iliskovic N. Doxorubicin-cardiomyopathy. N Engl J Med 1998;339: 900–5.
[20] Bristow MR, Mason JW, Billingham ME, Daniels JR. Dose–effect and structure–function relationships in doxorubicin cardiomyopathy. Am Heart J 1981;102: 709–18.
[21] Chalcroft SCW, Gavin JB, Herdson PB. Fine structural changes in rat myocardium induced by dunorubicin. Pathology 1973;5:99–105.
[22] Mettler FP, Young DM, Ward JM. Adriamycin-induced cardiotoxicity (cardiomyopathy and congestive heart failure) in rats. Cancer Res 1977;37:2705–13.
[23] Wakasugi S, Fischman AJ, Babich JW, et al. Myocardial substrate utilization and left ventricular function in adriamycin cardiomyopathy. J Nucl Med 1993;34:1529–35.
[24] Pye MP, Black M, Cobbe SM. Comparison of in vivo and in vitro haemodynamic function in experimental heart failure: use of echocardiography. Cardiovasc Res 1996;31:873–81.
[25] Schwarz ER, Pollick C, Dow J, Patterson M, Birnbaum Y, Kloner RA. A small animal model of non-ischemic cardiomyopathy and its evaluation by transthoracic echocardiography. Cardiovasc Res 1998;39:216–23.
[26] Xiang P, Deng HY, Li K, Huang GY, Chen Y, Tu L, et al. Dexrazoxane protects against doxorubicin-induced cardiomyopathy: upregulation of Akt and Erk phosphorylation in a rat model. Cancer Chemother Pharmacol 2009;63:343–9.
[27] Serrano J, Palmeira CM, Kuehl DW, Wallace KB. Cardioselective and cumulative oxidation of mitochondrial DNA following subchronic doxorubicin administration. Biochim Biophys Acta 1999;1411:201–5.
[28] Olson RD, Mushlin PS. Doxorubicin cardiotoxicity: analysis of prevailing hypotheses. FASEB J 1990;4:3076–86.
[29] Matsushita T, Okamoto M, Toyama J, Kodama I, Ito S, Fukutomi T, et al. Adriamycin causes dual inotropic effects through complex modulation of myocardial Ca^{2+} handling. Jpn Circ J 2000;64:65–71.
[30] Halili-Rutman I, Hershko C, Link G, Rutman AJ, Shainberg A. Inhibition of calcium accumulation by the sarcoplasmic reticulum: a putative mechanism for the cardiotoxicity of adriamycin. Biochem Pharmacol 1997;54:211–4.
[31] Szabadkai G, Rizzuto R. Participation of endoplasmic reticulum and mitochondrial calcium handling in apoptosis: more than just neighborhood? FEBS Lett 2004;567:111–5.
[32] Andersson KB, Birkeland JA, Finsen AV, Louch WE, Sjaastad I, Wang Y, et al. Moderate heart dysfunction in mice with inducible cardiomyocyte-specific excision of the *Serca2* gene. J Mol Cell Cardiol 2009;47:180–7.
[33] Trafford AW, Lederer WJ, Sobie EA. Keeping the beat: life without SERCA—is it possible? J Mol Cell Cardiol 2009;47:171–3.
[34] Fabritz L, Kirchhof P, Fortmüller L, Auchampach JA, Baba HA, Breithardt G, et al. Gene dose-dependent atrial arrhythmias, heart block, and Brady-cardiomyopathy in mice overexpressing A(3) adenosine receptors. Cardiovasc Res 2004;62:447–9.
[35] Bar-Yehuda S, Stemmer SM, Madi L, Castel D, Ochaion A, Cohen S, et al. The A3 adenosine receptor agonist CF102 induces apoptosis of hepatocellular carcinoma via de-regulation of the Wnt and NF-kappaB signal transduction pathways. Int J Oncol 2008;33:287–95.